Indian Journal of Chemistry
Vol. 48A, April 2009, pp. 473-479

Synthesis, crystal structures and protease activity of amino acid Schiff base iron(III) complexes

Mohammed S Ameerunisha Begum, Sounik Saha, Munirathinam Nethaji & Akhil R Chakravarty*

Department of Inorganic & Physical Chemistry, Indian Institute of Science, Bangalore 560 012, India
Email: arc@ipc.iisc.ernet.in

Received 23 January 2009; accepted 9 March 2009

Iron(III) complexes, $(NHEt_3)[Fe(III)(sal\text{-}met)_2]$ and $(NHEt_3)[Fe(III)(sal\text{-}phe)_2]$, of amino acid Schiff base ligands, viz., *N*-salicylidene-L-methionine and *N*-salicylidene-L-phenylalanine, have been prepared and their binding to bovine serum albumin (BSA) and photo-induced BSA cleavage activity have been investigated. The complexes are structurally characterized by single crystal X-ray crystallography. The crystal structures of the discrete mononuclear monoanionic complexes show FeN_2O_4 octahedral coordination geometry in which the tridentate dianionic amino acid Schiff base ligand binds through phenolate and carboxylate oxygen and imine nitrogen atoms. The imine nitrogen atoms are *trans* to each other. The Fe-O and Fe-N bond distances range between 1.9 and 2.1 Å. The sal-met complex has two pendant thiomethyl groups. The high-spin iron(III) complexes (μ_{eff} ~ 5.9 μ_B) exhibit quasi-reversible Fe(III)/Fe(II) redox process near -0.6 V vs. SCE in water. These complexes display a visible electronic band near 480 nm in tris-HCl buffer assignable to the phenolate-to-iron(III) charge transfer transition. The water soluble complexes bind to BSA giving binding constant values of ~10^5 M^{-1}. The complexes show non-specific oxidative cleavage of BSA protein on photo-irradiation with UV-A light of 365 nm.

Keywords: Bioinorganic chemistry, Protein binding, Protein cleavage, Crystal structure Amino acids, Iron

IPC Code: Int. Cl. [8] C07F15/04

Metal-based synthetic proteases are of importance as artificial peptidases and anti-metastasis agents[1-4]. Metal-based artificial nucleases have been extensively used in foot printing and therapeutic applications and as model restriction enzymes[5-10]. Among various synthetic metallonucleases, those showing photo-induced nuclease activity are of importance in photodynamic therapy (PDT) of cancer[11-15]. While PDT generally targets the primary tumors, compounds that regulate specific protein functions are of current interests for the development of new modality of cancer treatment, particularly targeted to secondary tumors generated from metastasis that leads the primary cancer cells becoming malignant. Metallopeptides are known to play an important role in peptide-nucleic acid chemistry related to transcription of DNA and related processes[16]. The present work stems from our interest to synthesize amino acid Schiff base complexes of iron(III) to explore their protein binding and protein cleavage activity. Ruthenium complexes like indazolium bis-indazoletetrachlororuthenate and $[(\eta^6\text{-}C_6H_5C_6H_5)Ru(en)Cl]^+$ (en = ethylenediamine) are used as new generation metal-based anti-cancer drugs to control tumor metastases[17,18]. We have designed two binary iron(III) complexes, $(NHEt_3)[Fe^{III}(sal\text{-}met)_2]$ (**1**) and $(NHEt_3)[Fe^{III}(sal\text{-}phe)_2]$ (**2**) of amino acid Schiff base ligands, viz., *N*-salicylidene-L-methionine (sal-met) and *N*-salicylidene-L-phenylalanine (sal-phe) to explore their protein binding and photo-induced protein cleavage activity using bovine serum albumin (BSA). Herein, we report the synthesis, crystal structures, BSA binding and BSA cleavage activity of the complexes **1** and **2**. The significant results of this work are the high BSA

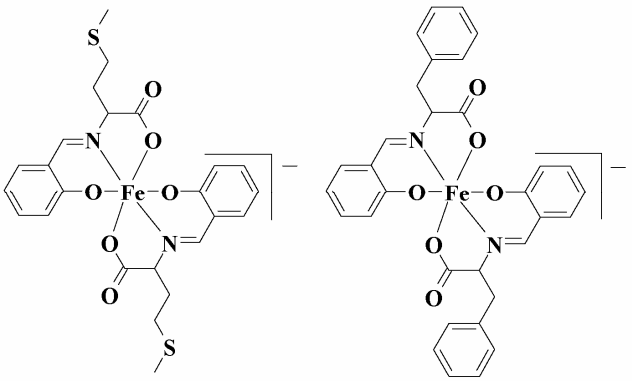

(1) **(2)**

binding propensity and UV-A light induced BSA cleavage activity of the complexes.

Materials and Methods

All the solvents and chemicals were purchased from Aldrich and S.D. Fine Chemicals (India). Bovine serum albumin (BSA), acrylamide, N,N-methylene bis-acrylamide, sodium dodecyl sulphate, ammonium persulphate, N,N,N′,N′-tetramethylethylenediamine were from Sigma-Aldrich. The elemental analyses were performed on PerkinElmer EA 2000 series instrument. ESI-MS spectrometric analysis was performed on a Hewlett Packard series 1100 MSD mass spectrometer. The electronic, infra red and fluorescence spectral measurements were conducted on Perkin Elmer Spectrum one 55, Perkin Elmer Lambda 35 and Perkin Elmer LS 50B spectrometers respectively. Cyclic voltammetric studies were carried out at 25 °C on a EG&G PAR (model 253) Versa Stat potentiostat /galvanostat provided with electrochemical analysis software 270 using glassy carbon working, platinum wire auxiliary and saturated calomel (SCE) reference electrodes. KCl and tetrabutylammonium perchlorate (TBAP) (0.1 *M* each) were used as supporting electrolytes in water and DMF respectively. Room temperature magnetic susceptibility data were obtained using Lewis-coil-force magnetometer (model 300) of George Associates Inc. $Hg[Co(NCS)_4]$ was used as a standard and the diamagnetic corrections were made in the susceptibility data[19]. The ligands, (H_2sal-met, *N*-salicylidene-L-methionine; H_2sal-phe, *N*-salicylidene-L-phenylalanine) were prepared by following a reported procedure[20].

Synthesis of $(NHEt_3)[Fe(sal\text{-}met)_2]$ (1) and $(NHEt_3)[Fe(sal\text{-}phe)_2]$ (2)

The complexes were prepared by a general method in which the ligand (H_2sal-met, 0.51 g; H_2sal-phe, 0.54 g; 2 mmol) was reacted with $FeCl_3$ (0.16 g, 1 mmol) in methanol (30 mL) in the presence of Et_3N (0.2 mL, 2 mmol) and the reaction mixture was heated under reflux for 3 h. The solution was filtered while hot and evaporated on a rotary evaporator to obtain a residue that was dissolved in methanol (20 mL), and filtered. The product was precipitated as a reddish brown powder on addition of ethyl acetate (80 mL). Single crystals suitable for X-ray diffraction were obtained on crystallization of the complex from CH_2Cl_2-hexane mixture. Yield: 0.3 g (44%) for **1** and 0.2 g (27%) for **2**. Anal: Calc. for $(NHEt_3)[Fe(sal\text{-}met)_2].H_2O$, $FeC_{30}H_{44}N_3O_7S_2$: C, 53.09 H, 6.53, N, 6.19%. Found: C, 52.90, H, 6.78, N, 6.32. ESI-MS in MeCN): 661.2 $\{[Fe(sal\text{-}met)_2] + (Et_3NH) + H\}^+$. FT-IR (KBr disc), ν ($cm^{-1}$): 3438br, 2937w, 2735w, 2677w, 2494w, 1623s, 1600s, 1440m, 1262m, 1144m, 804s, 757m, 550m (br, broad, w, weak, s, strong, m, medium). UV-visible in tris-HCl buffer (*p*H 7.2): λ (nm)/ε (M^{-1} cm^{-1}): 485 (4400), 418 (3700), 316 (13600), 294 (13900), 263 (40000), 235 (54700). $E_{1/2}$, in water (0.1 *M* KCl): -0.57 V vs. SCE [Δ*E*p: 135 mV at 50 mV s^{-1}]. Conductivity in DMF: 80 S m^2 M^{-1}. μ_{eff}: 5.8 μ_B. Anal.: Calc. for $(NHEt_3)[Fe(sal\text{-}phe)_2].2H_2O$, $FeC_{38}H_{46}N_3O_8$: C, 62.64, H, 6.36, N, 5.77%. Found: C, 62.62, H, 6.65, N, 6.07. ESI-MS in MeCN: 693.4 $\{[Fe(sal\text{-}phe)_2] + (Et_3NH) + H\}^+$. FT-IR (KBr disc), ν ($cm^{-1}$): 3430br, 2928w, 2678w, 2494w, 1625s, 1600s, 1542m, 1448m, 1307m, 1150m, 1030m, 769m, 703m, 548m. UV-visible in tris-HCl buffer (*p*H 7.2): λ (nm)/ε ($M^{-1}cm^{-1}$): 482 (3700), 420 (3100), 316 (13500), 293 (13700), 262 (38100), 235 (53700). $E_{1/2}$ in water (0.1 *M* KCl): -0.62 V vs. SCE (Δ*E*p: 230 mV at 50 mV s^{-1}). Conductivity in DMF: 80 S m^2 M^{-1}. μ_{eff}: 5.9 μ_B. The complexes were soluble in water, MeOH, MeCN, DMF and CH_2Cl_2.

X-ray crystallography

The structures of the complexes **1** and **2** were determined by X-ray crystallography. Single crystals of **1** were obtained on slow evaporation of the CH_2Cl_2-hexane (1:1 *v*/*v*) solution at ~4 °C. Single crystals of **2** were obtained in a similar way but at an ambient temperature. Red crystals of **1** and **2** were mounted on glass fibers using epoxy cement. The data were collected at 25 °C on an automated Bruker SMART APEX CCD diffractometer with Mo Kα X-ray source (λ = 0.71073 Å). Data reductions and absorption corrections were done using SAINT and SADABS software programs[21]. The structures were solved and refined using SHELX programs package[22]. Non-hydrogen atoms were refined anisotropically. Hydrogen atoms were fixed at their calculated positions and refined using a riding model. Crystallographic data for complexes are given in Table 1.

Protein binding and cleavage

The interactions of the complexes with the bovine serum albumin (BSA) were investigated in phosphate buffer medium (*p*H 7.2) containing DMF (5%) using the quenching of the intrinsic fluorescence of BSA upon ligand binding[23]. To a 2 μ*M* solution of BSA, increasing concentrations of the complexes **1/2** were

Table 1 — Selected crystallographic data and structure refinement for complexes **1** and **2**

Complex	**1**	**2**
Formula	$C_{30}H_{42}FeN_3O_6S_2$	$C_{38}H_{38}FeN_3O_7$
FW(g/mol)	660.64	704.56
Space group	$P2_12_12_1$	$P2_1$
a (Å)	10.542(3)	11.867(3)
b (Å)	17.212(6)	11.558(3)
c (Å)	18.404(6)	14.128(4)
α(°)	90	90
β(°)	90	105.140(4)
γ(°)	90	90
V (Å^3)	3339.2(19)	1870.5(9)
Z	4	2
T (K)	293(2)	293(2)
λ (Å) (Mo - K_α)	0.71073	0.71073
μ(Mo−K_α) (mm^{-1})	0.620	0.453
ρ_{calc} (g cm^{-3})	1.314	1.251
F(000)	1396	738
Parameters	379	442
Restraints	0	1
Goodness-of-fit on F^2	1.010	1.050
Unique reflections	6546	7466
Observed reflections [$I > 2\sigma(I)$]	3126	5396
$R1$ (obs.) ($R1$, all data)[a]	0.0777 (0.1780)	0.0609 (0.0880)
$wR2$ ($wR2$, all data)[b]	0.1459 (0.1829)	0.1345 (0.1480)

[a] $R = \Sigma||F_o|-|F_c||/\Sigma|F_o|$, [b] $wR = \{\Sigma[w(F_o^2-F_c^2)^2]/\Sigma[w(F_o)^2]\}^{½}$, where $w = 1 / [\sigma^2(F_o^2) + (0.0500P)^2 + 0.0P]$ and $P = (F_o^2 + 2F_c^2)/3$.

added. The fluorescence spectra were recorded after each addition using PerkinElmer LS50B fluorescence spectrophotometer set at 285 nm excitation and 344 nm emission. The binding constants of the complexes with BSA were determined from a linear fit of the data (Origin 6.1) using the Stern-Volmer equation: $(I_0/I) = K_{SV}$ x [complex] + 1, where I_0 is the fluorescence intensity of BSA in absence of the complexes and I is the fluorescence intensity after addition of the complexes, K_{SV} is the Stern-Volmer quenching constant or the binding constant and [complex] is the complex concentration.

The photocleavage of BSA by the iron(III) complexes **1** and **2** (125-500 μM) was studied by denaturing sodium dodecyl sulphate polyacrylamide gel electrophoresis (SDS PAGE)[24,25]. The protein cleavage experiments were done in a dark room at 25 ºC using BSA (5 μ*M*) in 50 m*M* tris-HCl buffer (*p*H 7.2) and the complex (2 μL). The concentration of the complexes in DMF or the additives in buffer corresponded to the quantity in 10 μL stock solution after dilution to the 50 μL final volume using tris-HCl buffer. The samples were incubated for 1 h at 37 ºC,

Table 2 — Physicochemical and BSA-binding data for the complexes **1** and **2**

Complex	**1**	**2**
λ_{max}(nm)(ε/M^{-1}cm^{-1})[a]	485(4400), 418(3700)	482(3700), 420(3100)
$E_{1/2}$/V (ΔE_p/mV)[b]	-0.57 (135)	-0.62 (230)
μ_{eff}[c] (BM)	5.8	5.9
K_{SV}[d] (M^{-1})	1.91×10^5	2.98×10^5

[a] In tris-HCl buffer (5 m*M*, *p*H 7.2).
[b] Fe(III)/Fe(II) couple in water-0.1 *M* KCl. Potentials are versus SCE at a scan rate 100 mV s^{-1}.
[c] Magnetic moment at 298 K. [d] Binding constant with BSA.

followed by exposure to UV-A light (100 W). After exposure, the samples were evaporated to dryness using EYELA centrifugal vaporizer, followed by addition of 5X loading buffer containing 10% SDS. The samples were then boiled for 3 min to denature the protein completely. The solutions were finally loaded into the wells of 10%/3% (separating/stacking) polyacrylamide gel with prestained molecular weight marker (Bangalore Genei) for approximate molecular weight determination. Electrophoresis was carried out in a dark room in SDS PAGE running buffer at 60 V until the samples entered the stacking gel completely and thereafter the voltage was increased to 100 V until the dye font reached the bottom of the gel. The gels were stained with Coomassie Brilliant Blue R-250 in a mixture of MeOH, H_2O and acetic acid (2:7:1 *v*/*v*). Destaining was carried out in MeOH, H_2O and acetic acid mixture (5:4:1 *v*/*v*). The inhibition reactions were carried out adding different reagents (TEMP 0.5 m*M*, NaN_3, 0.5 m*M*; KI, 0.5 m*M*, EtOH, 10 μl) to BSA prior to the addition of the complex (500 μ*M*).

Results and Discussion

Synthesis of the complexes

Binary iron(III) complexes $(NHEt_3)$[Fe(III)(sal-met)$_2$] (**1**) and $(NHEt_3)$[Fe(III)(sal-phe)$_2$] (**2**) of amino acid Schiff base ligands, viz., *N*-salicylidene-L-methionine (sal-met) and *N*-salicylidene-L-phenylalanine (sal-phe), were prepared from the reaction of the Schiff bases and $FeCl_3$ in the presence of Et_3N. The complexes were characterized from analytical and spectral data (Table 2). The IR spectra of the complexes exhibit characteristic IR bands near 1620 cm^{-1} and 1600 cm^{-1} that are assignable to the coordinated ν_{COO} and $\nu_{CH=N}$ stretching vibrations. The presence of triethylammonium cations in **1** and **2** is evidenced from the IR spectra showing weak bands in the range of 2900 – 2400 cm^{-1}. The complexes show ESI-MS molecular ion peaks at *m*/*z* values of 661 (100%) and 693 (100%). The high-spin d^5-Fe(III)

complexes are redox active showing quasi-reversible one-electron Fe(III)/Fe(II) redox process near –0.6 V vs. SCE in water (0.1 *M* KCl) (Fig. 1). The UV-visible spectra of the complexes in tris-HCl buffer (5m*M*, *p*H 7.2) show visible bands near 480 nm and 420 nm (Fig. 1). The 480 nm band is assignable to the phenolate-to-iron(III) charge transfer band[26,27].

Crystal structures of the complexes

The structures of the complexes were determined by X-ray crystallography. The ORTEP diagrams are shown in Figs 2 and 3. Selected bond distances and angles are given in Table 3. Complex **1** crystallizes in the orthorhombic space group $P2_12_12_1$ with four molecules in the unit cell. The crystal structure shows the presence of $[Fe(sal\text{-}met)_2]^-$ and triethylammonium cation in a 1:1 ratio. The Fe(III) center is octahedrally coordinated having two Schiff base ligands each coordinating through the imine nitrogen, phenolate oxygen and carboxylate oxygen atom giving a FeN_2O_4 coordination. The imine moieties in the structure are *trans* to each other. The thiomethyl group of the Schiff base ligand is pendant without showing any bonding with the metal center. The Fe-N and Fe-O bond distances range between 1.912(5) to 2.090(6)Å. The complex displays chemically significant H-bonding interactions ($NH^{\cdots}O$=C, 2.892 Å) involving triethylammonium

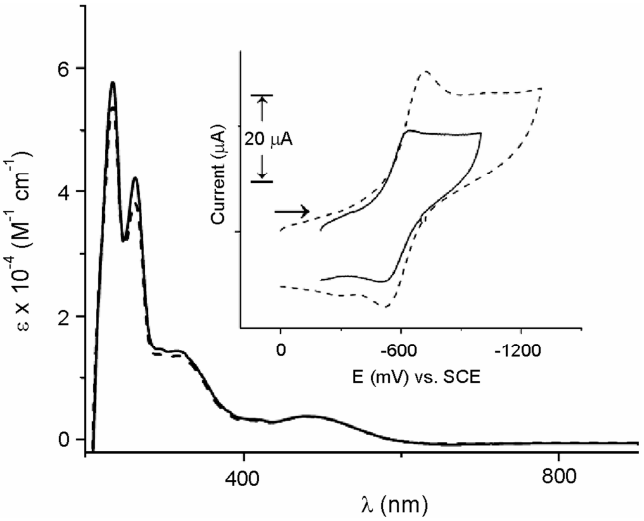

Fig. 1 — Electronic spectra of the complexes **1** (—) and **2** (---) in tris-HCl buffer (5 m*M*, *p*H 7.2). The inset shows the voltammetric responses of the complexes **1** (—) and **2** (---) in H_2O-0.1 *M* KCl.

Table 3 — Selected bond lengths (Å) and bond angles (º) in **1** and **2** with esds in parentheses

1		**2**	
Bond lengths			
Fe(1)-N(1)	2.089(5)	Fe(1)-N(1)	2.097(3)
Fe(1)-N(2)	2.090(6)	Fe(1)-N(2)	2.108(3)
Fe(1)-O(1)	1.932(5)	Fe(1)-O(1)	1.911(3)
Fe(1)-O(3)	2.024(5)	Fe(1)-O(3)	2.093(3)
Fe(1)-O(4)	1.912(5)	Fe(1)-O(4)	1.914(3)
Fe(1)-O(6)	2.022(6)	Fe(1)-O(5)	2.048(3)
Bond angles			
O(1)-Fe(1)-O(3)	163.1(2)	O(1)-Fe(1)-O(3)	161.26(13)
O(4)-Fe(1)-O(6)	165.3(2)	O(4)-Fe(1)-O(5)	162.10(13)
N(1)-Fe(1)-N(2)	165.3(2)	N(1)-Fe(1)-N(2)	172.91(13)
O(1)-Fe(1)-O(6)	90.3(2)	O(1)-Fe(1)-O(5)	92.22(14)
O(4)-Fe(1)-O(1)	92.3(2)	O(1)-Fe(1)-O(4)	96.87(13)
O(6)-Fe(1)-O(3)	88.7(2)	O(4)-Fe(1)-O(3)	91.81(13)
O(4)-Fe(1)-N(1)	106.1(2)	O(5)-Fe(1)-O(3)	84.21(13)
O(1)-Fe(1)-N(1)	85.8(2)	O(1)-Fe(1)-N(1)	86.27(14)
O(6)-Fe(1)-N(1)	88.5(2)	O(4)-Fe(1)-N(1)	96.96(14)
O(3)-Fe(1)-N(1)	77.2(2)	O(5)-Fe(1)-N(1)	99.00(12)
O(4)-Fe(1)-O(3)	92.8(2)	O(3)-Fe(1)-N(1)	76.17(14)
O(4)-Fe(1)-N(2)	87.6(2)	O(1)-Fe(1)-N(2)	99.80(15)
O(1)-Fe(1)-N(2)	99.33(19)	O(4)-Fe(1)-N(2)	86.01(13)
O(6)-Fe(1)-N(2)	77.8(2)	O(5)-Fe(1)-N(2)	77.24(13)
O(3)-Fe(1)-N(2)	97.0(2)	O(3)-Fe(1)-N(2)	97.35(14)

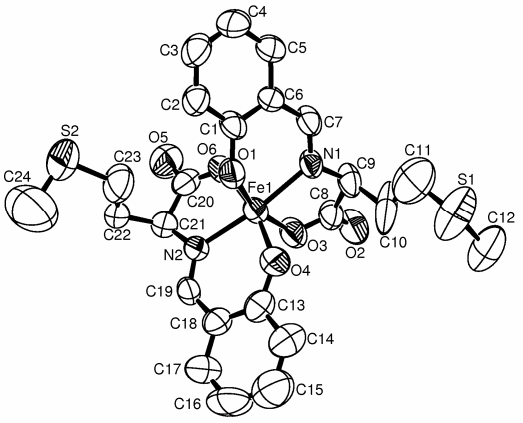

Fig. 2 — The ORTEP view of the complex anion in $(NHEt_3)[Fe(sal\text{-}met)_2]$ (**1**) with 50% probability thermal ellipsoids and atom numbering scheme.

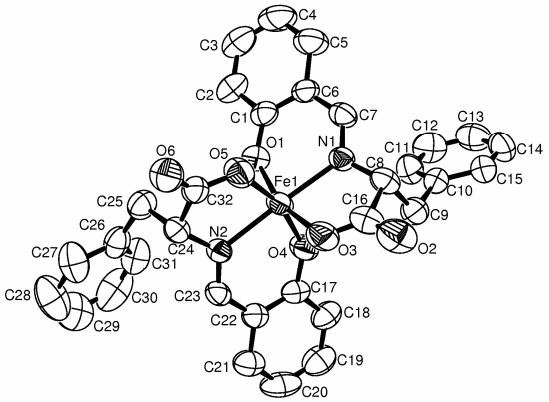

Fig. 3 — The ORTEP view of the complex anion in $(NHEt_3)[Fe(sal\text{-}phe)_2]$ (**2**) with 50% probability thermal ellipsoids and atom numbering scheme.

cation and the carbonyl group of the Schiff base ligand. Complex **2** crystallizes in the monoclinic space group $P2_1$ with lattice solvent water molecules. The structure of $[Fe(sal\text{-}phe)_2]^-$ shows the presence of an iron(III) center that is octahedrally coordinated to two sal-phe ligands giving FeN_2O_4 coordination. The structural features of two complexes are essentially similar. Complex **2** shows intermolecular H-bonding interactions involving water and carbonyl groups of Schiff base [O(2)…O(7), 2.820 Å; O(6)…O(7), 2.866 Å].

BSA protein binding study

To investigate whether the anionic iron(III) complexes **1** and **2** bind to the model protein BSA, fluorescence measurements were carried out. The conformational changes of BSA were evaluated by the measurement of intrinsic fluorescence intensity of protein before and after addition of the complexes. Fluorescence data generally give information about the molecular environment in the vicinity of the chromophore molecules[23]. Addition of the DMF solutions of the complexes decreased the emission intensity of BSA at 344 nm in phosphate buffer (*p*H 7.2). Addition of the complexes **1** and **2** shows a concentration-dependent quenching of the intrinsic fluorescence of BSA, without changing the emission maximum, indicating that the complexes bind to BSA without altering the local dielectric environment. The plot of the emission intensities (I/I_0) against the complex concentrations is shown in Fig. 4. The K_{SV} values of the complexes **1** and **2** were calculated from the slope of the plot of I_0/I versus [complex] (Table 2). The binding constant values of ~10^5 M^{-1} suggest moderate binding propensity of the complexes to BSA.

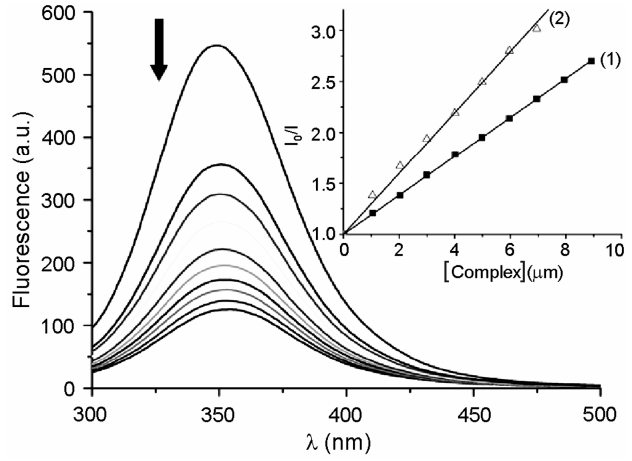

Fig. 4 — Effect of increasing concentrations of the complexes **1** (Δ) and **2** (■) on the emission intensity of bovine serum albumin (BSA) in phosphate buffer (*p*H 7.2).

The higher binding affinity of the complex **2** is attributed to the presence of the pendant aromatic residues.

BSA protein photocleavage study

The protein photocleavage activity of the complexes **1** and **2** (125-500 μ*M*) was investigated at 365 nm and analyzed on a 10%/3% SDS-PAGE in tris-HCl (50 m*M*, *p*H 7.2). The SDS PAGE gels are shown in Figs 5 and 6. A 500 μ*M* solution of complexes **1** or **2**

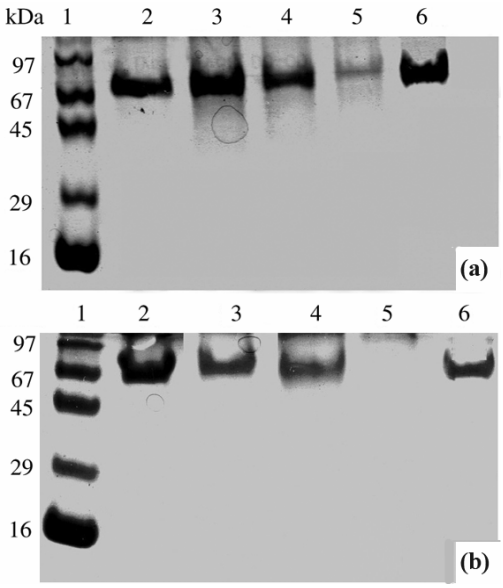

Fig. 5 — SDS PAGE gel diagram showing the photocleavage of BSA (5 μ*M*) by the complexes **1** and **2** (500 μ*M*) at 365 nm excitation for 1 h (for the lanes 2-5) in tris HCl/NaCl buffer (50 m*M*, *p*H 7.2); lane 6 is without any photoexposure. [(a) lane-1 molecular weight marker, lane-2 BSA control, lane-3 BSA + **1** (125 μ*M*), lane-4 BSA + **1** (250 μ*M*), lane-5 BSA + **1** (500 μ*M*), lane-6 BSA + **1** (500 μ*M*) in dark; (b) lane-1 molecular weight marker; lane-2 BSA control; lane-3 BSA + **2** (125 μ*M*); lane-4 BSA + **2** (250 μ*M*); lane-5 BSA + **2** (500 μ*M*); lane-6 BSA + **2** (500 μ*M*) in dark].

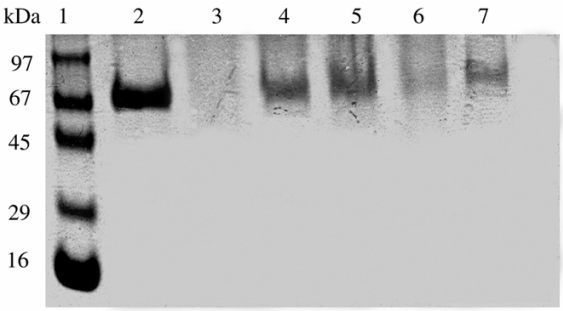

Fig. 6 — SDS PAGE gel diagram showing the mechanistic aspects of BSA (5 μ*M*) photocleavage by complex **1** (500 μ*M*) at 365 nm excitation for 1 h photoexposure using various additives. [lane-1 molecular weight marker; lane-2 BSA control; lane-3 BSA + **1**; lane-4 BSA + **1** + KI (0.5 m*M*); lane-5 BSA + EtOH (10 μL); lane-6 BSA + TEMP (0.5 m*M*); lane-7 BSA + NaN_3 (0.5 m*M*)].

completely cleaves BSA into smaller fragments that are not observable by SDS PAGE. Decrease in the intensity of the BSA band at ~66 kD was observed. This results from non-specific cleavage of the protein by the highly diffusible $^{\bullet}OH$ radicals generated by the complexes upon photoexcitation at 365 nm UV-A light[1,28]. Moreover, complex **2** showed higher cleavage activity than **1** due to greater binding of **2** over **1** with BSA. The protein cleavage activity enhances with an increase in the concentration of the complexes (Fig. 6).

The generation of hydroxyl radical was observed from the mechanistic studies using KI, EtOH, DMSO as hydroxyl radical scavengers and TEMP, DABCO and NaN_3 as singlet oxygen quenchers. Addition of the hydroxyl radical scavengers prior to the exposure to UV-A light inhibited the photocleavage reaction as can be seen from the intense band as compared to that without addition of the inhibitors. Singlet oxygen quenchers, on the other hand, were unable to inhibit the photocleavage reaction. The photo-excitation is believed to generate reactive iron(II) species from a photo-redox mechanism with subsequent activation of molecular oxygen to form superoxide anion radical that converts to hydroxyl radicals in the reaction: $3O_2^{\bullet-} + 2H^+ \rightarrow {}^{\bullet}OH + HO^- + 2O_2$, as known for antitumor agent podophyllotoxin[26,29].

Conclusions

Amino acid Schiff base complexes of iron(III) are prepared, structurally characterized and their protein binding and cleavage activity studied. The complexes show good BSA protein binding propensity. The complexes which are inactive in showing any protein cleavage activity in dark, exhibit significant photo-induced protein cleavage activity in UV-A light of 365 nm following a mechanistic pathway involving formation of hydroxyl radicals. Iron being a bio-essential metal ion, the present results are of importance towards designing iron-based amino acid/peptide complexes as new anti-metastasis agents for targeted treatment of secondary (malignant) tumors. Further work in this direction is in progress.

Supplementary Data

CCDC 715347 and 715348 contain the supplementary crystallographic data that can be obtained free of charge from the Director, CCDC, 12 Union road, Cambridge, CB2 1EZ, UK (Fax: +44 1223 336 033, Email: deposit@ccdc-cam.ac.uk or www:http://www.ccdc.cam.ac.uk).

Acknowledgement

We thank the Department of Science and Technology (DST), Government of India and the Council of Scientific and Industrial Research (CSIR), New Delhi, for financial support [SR/S5/MBD-02/2007 and 01(2081)/06/EMR-II]. We also thank the Alexander von Humboldt Foundation, Germany, for the donation of an electrochemical system. MSAB and SS thank CSIR for fellowship under the Scientist Pool Scheme and research fellowship, respectively. ARC thanks DST for JC Bose National Fellowship.

References

1 Tanimoto S, Matsumura S & Toshima K, *Chem Commun,* (2008) 3678.

2 Rajendiran V, Palaniandavar M, Swaminathan P & Uma L, *Inorg Chem,* 46 (2007) 10446.

3 Kumar C V, Buranaprapuk A, Opitech G J, Moyer M B, Jockusch S & Turro N J, *Proc Natl Acad Sci USA*, 95 (1998) 10361.

4 Bergamo A & Sava G, *Dalton Trans,* (2007) 1267.

5 Sigman D S, *Acc Chem Res,* 19 (1986) 180.

6 Burrows C J & Muller J G, *Chem Rev,* 98 (1998) 1109.

7 Sreedhara A & Cowan J A, *J Biol Inorg Chem,* 6 (2001) 337.

8 Wolkenberg S E & Boger D L, *Chem Rev,* 102 (2002) 2477.

9 Schultz P G & Dervan P B, *J Am Chem Soc,* 105 (1983) 7748.

10 Erkkila K E, Odom D T & Barton J K, *Chem Rev,* 99 (1999) 2777.

11 Detty M R, Gibson S L & Wagner S J, *J Med Chem,* 47 (2004) 3897.

12 Chifotides H T & Dunbar K R, *Acc Chem Res,* 38 (2005) 146.

13 Boerner L J K & Zaleski J M, *Curr Opin Chem Biol,* 9 (2005) 135.

14 Bonnett R, *Chemical Aspects of Photodynamic Therapy*, (Gordon & Breach, London, UK), 2000.

15 Henderson B W, Busch T M, Vaughan L A, Frawley N P, Babich D, Sosa T A, Zollo J D, Dee A S, Cooper M T, Bellnier D A, Greco W R & Oseroff A R, *Cancer Res,* 60 (2000) 525.

16 Hlavaty J J & Nowak T, *Biochemistry*, 36 (1997) 15514.

17 Yan Y K, Melchart M, Habtemariam A & Sadler P J, *Chem Commun*, (2005) 4764.

18 Hartinger C G, Zorbas-Seifried S, Jakupec M A, Kynast B, Zorbas H & Keppler B K, *J Inorg Biochem,* 100 (2006) 891.

19 Kahn O, *Molecular Magnetism* (VCH, Weinheim, Germany), 1997.

20 Heinert D & Martell A E, *J Am Chem Soc,* 84 (1962) 3257-3263.

21 *SAINT (ver. 6.02), SHELXTL (6.10), SADABS (Ver. 2.03)* (Bruker AXS Inc., Madison, Wisconsin, USA) 2002.

22 Sheldrick M, *SHELX-97, Program for Crystal Structure Solution and Refinement* (University of Göttingen, Göttingen, Germany) 1997.

23 Quiming N S, Vergel R B, Nicolas M G & Villanueva J A, *J Health Sci,* 51 (2005) 8.

24 Schägger H & von Jagow G, *Anal Biochem*, 166 (1987) 368.

25 Kumar C V, Buranaprapuk A, Sze H C, Jockusch S & Turro N J, *Proc Natl Acad Sci USA,* 99 (2002) 5810.

26 Roy M, Saha S, Patra A K, Nethaji M & Chakravarty A R, *Inorg Chem*, 46 (2007) 4368.

27 Kraft B J & Zaleski J M, *New J Chem*, 25 (2001) 1281.

28 Jones G B, Wright J M, Hynd G, Wyatt J K, Yancisin M & Brown M A, *Org Lett*, 2 (2000) 1863.

29 Sakurai H, Miki T, Imakura Y, Shibuya M & Lee K-H, *Mol Pharmacol*, 40 (1991) 965.